Motion Planning of Fully-actuated Closed Kinematic Chains with Revolute Joints: A Comparative Analysis

Avishai Sintov, Andy Borum, and Timothy Bretl

***Abstract*—This paper provides a comparative analysis of common strategies for sampling-based motion planning of fully-actuated closed kinematic chains with revolute joints. Three strategies are reviewed: singularity sampling, swapping between possible passive chains while using the active-passive chains kinematic approach and using Newton-Raphson projections. The strategies are compared using analytical and empirical results. Various measures, such as sampling time and visibility, are used to analyze the strategies in several dual-arm planning problems using the three different planning algorithms. This comparative analysis provides insight into the strengths and weaknesses of each sampling strategy. Results indicate that the kinematic-based passive chains swapping strategy is more preferable in environments with obstacles but harder to implement for various robotic arms.**

***Index Terms*—Manipulation Planning, Dual Arm Manipulation**

I. Introduction

In robotics, systems of *closed kinematic chains* (CKC) appear in many applications such as dual arm manipulation [1], gait [2], grasping, and multiple mobile robots manipulating an object [3]. The motion planning problem for CKC systems is to find a path from start to goal configurations that satisfies joint limits, is collision-free, and satisfies a set of closure constraints. Finding a path that satisfies the closure constraints is considered a hard problem due to the low dimensionality of the constraint manifold in the ambient configuration space [4]. In addition, explicit descriptions of this manifold are usually not available. Thus, the probability of sampling a point that satisfies the closure constraint is null [5]. Consequently, sampling-based approaches excelling in high-dimensional problems [6] cannot be directly applied to such problems and must embrace additional methods to ensure a feasible path.

In the context of sampling-based motion planning, the common approach for sampling a configuration that satisfies the closure constraint is through *projection* [7]. In this way, a random configuration in the ambient space is projected onto the constraint surface. The major challenge, however, is to enable geodesic traverse across the manifold between projected configurations (i.e., enable local-connections). A projection-based local planning approach deforms a straight line connecting two configurations onto the manifold [8], [9]. Recent work improved this simple projection approach by proposing tangent-space based strategies [10]. The Tangent-Bundle-RRT (TB-RRT) [11] expands a tree over overlapping tangent bundles approximating the manifold. By doing so, the planning is able to generate samples close to the manifold while deferring projections until necessary. Similarly, the AtlasRRT [12] incrementally constructs a set of minimally overlapping tangent spaces (atlas) on the manifold. A tree is expanded by sampling new points on the tangent spaces followed by projection. However, in this paper we wish to focus on projection-based planning methods as these are the most commonly used and straight-forward to implement approaches.

Projection methods, which are also used for geodesic local-connection, are commonly divided into two catagories, numerical (or optimization) -based [7], [13] and analytical (or inverse-kinematics) -based [14], [15]. One might assume that analytical methods perform better than numerical methods due to the additional computational cost. In this paper, we wish to challenge this assumption and determine which is the favorable method for planning with fully- actuated CKC. Therefore, the main objective of this paper is to review several methods within the context of sampling-based planning. This review provides insight into the strengths and weaknesses of each strategy and may assist in future choices for motion planning of CKC. Thus, we identify prominent projection-based strategies for the motion planning of CKC, and conduct a comparative analysis. Some of the strategies have been known in the professional community, but, to the best of our knowledge, never been addressed properly in literature. We discuss these methods here and contribute some additional insights.

It is worth mentioning early work of sampling-based planning for CKC. Seminal work in [5] used an optimization-based approach applied to the Probabilistic Roadmap (PRM) and later extended to the Rapidly-exploring Random Tree (RRT) [13]. They used randomized gradient descent to minimize closure residual functions and converge samples to the surface. Later in [16], relaxation of the constraint was introduced by

Manuscript received: Feb., 6, 2018; Revised April, 15, 2018; Accepted June, 1, 2018.

This paper was recommended for publication by Editor John Wen upon evaluation of the Associate Editor and Reviewers' comments. This work was supported by the NSF under Grant No. IIS-1320519. (Corresponding author: Avishai Sintov.)

A. Sintov is with the Coordinated Science Laboratory, University of Illinois at Urbana-Champaign, Urbana, IL, 61801, USA. e-mail: asintov@illinois.edu.

A. Borum and T. Bretl are with the Department of Aerospace Engineering, University of Illinois at Urbana-Champaign, Urbana, IL, 61801, USA. e-mail: {borum2,tbretl}@illinois.edu.

Digital Object Identifier (DOI): .

reformulating the equality constraint to an inequality with a small tolerance. In [17], the closure constraint was relaxed by adding joint compliance yielding a feasible sampling volume over the manifold. These relaxation approaches enable direct sampling in the relaxed volume. Thus, projection is not required. However, these approaches suffer from high planning time and may cause implementation problems such as damaging forces.

The number of samples and the cost of checking a local-connection are obviously important measures in the performance of a planner. These measures are determined by the chosen method of projection. Equally important is the probability of two configurations being connected with a single local-connection. This probability, derived from the notion of *visibility* [18], is also determined by the projection and local-connection strategies and is critical to the performance. For some of the reviewed methods, we provide an upper limit for this probability. These measures are the basis of our comparative analysis for closed kinematic chains problems.

II. Preliminaries

In this section we define the planning problem for closed kinematic chains and review some relevant fundamentals in constrained sampling-based planning.

A. Problem definition

Let $\mathcal{R}$ denote an n-dimensional CKC with $n-1$ rigid links connected by n revolute and actuated joints in the Euclidean space $\mathbb{R}^d$, where $d=2$ or $d=3$ in the planar and spatial case, respectively. Further, denote $\mathcal{C}$ as the configuration space of $\mathcal{R}$ formed by its joint space product. The kinematic closure constraint can generally be expressed as a system of n_c non-linear equations $C(\phi)=0$ where $n_c=3$ or $n_c=6$ for planar or spatial problems, respectively, and $\phi \in \mathcal{C}$. Hence, the set of all configurations of $\mathcal{R}$ satisfying the closure constraint is the subset

$$\mathcal{C}_{cl} = \{\phi \in \mathcal{C} : C(\phi) = 0\}. \tag{1}$$

Further, let $\mathcal{C}_b \subset \mathcal{C}$ be a restricted region due to obstacles and joint limits, and let the free configuration space of $\mathcal{R}$ be $\mathcal{C}_{free} = \mathcal{C} \setminus \mathcal{C}_b$. Therefore, the feasible set $\mathcal{C}_o$, defined as

$$\mathcal{C}_o = \{\phi \in \mathcal{C} : \phi \in \mathcal{C}_{free} \cap \mathcal{C}_{cl}\}, \tag{2}$$

is the set of configurations that satisfy the closed kinematic chain constraint, satisfy joint limits and are collision-free. When referring to a real-life example of two manipulators holding an object (as in Figure 2), we assume that the object and grippers form a rigid body, thus, forming one closed chain.

The motion planning problem is as follows. Given start and goal configurations $\phi_s \in \mathcal{C}_o$ and $\phi_g \in \mathcal{C}_o$ of the system $\mathcal{R}$, find a continuous path $\alpha : [0,1] \to \mathcal{C}_o$ such that $\alpha(0)=\phi_s$ and $\alpha(1)=\phi_g$.

B. Projection methods

Constraints such as (1) reduce the configuration space to a lower-dimensional subset in the ambient space [4]. Thus, the probability of sampling a valid configuration on the closure constraint surface tends to be zero. The common approach is to sample a random configuration in the ambient space and then project it onto the constraint surface [8]. The two prominent approaches for projection are the *active and passive chains* (APC) method and the *Newton-Raphson* (NR) method, and are presented in this section.

1) Active and passive chains: A well known approach for generating a random configuration that satisfies the closed chain constraint is breaking $\mathcal{R}$ into two open subchains [14]: the active chain $\mathcal{R}_a$ and the passive chains $\mathcal{R}_p$. The active chain configuration is sampled uniformly and then inverse kinematics (IK) is used to enforce, if possible, the closure constraint on the remaining passive chain. It is important to note that there are no real passive joints in the chain and the declaration of a set of joints as a passive chain is solely performed for configuration calculations and planning purposes. However, this approach introduces artificial singularities as later discussed. Although not exactly a projection operation, we still refer to APC as such as commonly done in the literature [10]. Since the configuration of $\mathcal{R}_a$ is randomly sampled, its dimension results solely from restrictions on the passive chains. Most importantly, the passive chain must be non-redundant to enable closed-form IK solutions [4]. In addition, it is preferable that the passive chain have enough joints in a formation such that its tip is fully actuated to any position and orientation in the workspace. A passive chain where the number of joints is smaller than the number of degrees-of-freedom (DOF) of the end-effector could significantly increase the projection time of a valid configuration and can be infeasible for motion planning. Normally, the passive chains of spatial systems would be chosen to have an *elbow-wrist* formation [19] (six DOF) ensuring full actuation.

2) Newton-Raphson projection: In the Newton-Raphson (NR) approach described in [9], a configuration in the ambient space is numerically projected onto the constraint surface. Starting from a randomly sampled configuration, the Newton-Raphson method is used to reduce the residual of the constraint error $\|C(\phi)\|$. At each iteration, the pseudo-inverse of the Jacobian matrix of the constraint is calculated and used to take a step in the configuration space to reduce the constraint residual. This repeats until the residual of the constraint is below some tolerance or the number of iterations reaches an upper bound. Backtracking line search can be used to expedite convergence by calculating the maximum step size.

A preliminary experimental comparison of the two projection methods with regards to the projection distance was performed. 500,000 random configurations were projected for two spatial robotic arms of six DOF each (as seen in Figure 2b) holding an object, without joint limits and collision avoidance. The results show that APC runtime is three to six times faster than NR and, as expected, does not depend on the projection distance. Using NR, the number of iterations required for convergence increases with projection distance. Although APC has better runtime, not all selections of active chains can be be closed with the IK of the passive chain. In this experiment, the APC success rate is 7.92% compared to 100% for NR.

C. Local-connection

A straight line connecting two valid configurations is unlikely to be contained in $\mathcal{C}_{cl}$. Thus, a local connection that traverse the surface of the constraint must be found. Projecting interpolated points from a path connecting two configurations onto the manifold may raise continuity problems. Thus, the Recursive Bi-Section (RBS) technique proposed in [9] provides an efficient way to discretely deform a straight line onto $\mathcal{C}_{cl}$. The mid-point of the two configurations is first projected onto $\mathcal{C}_{cl}$ and checked to ensure it also lies in $\mathcal{C}_o$. If the mid-point is valid, the algorithm is repeated on each of the formed segments until a desired resolution is met or failure to project on $\mathcal{C}_o$ occurs. This method was later extended to trajectory optimization of constrained systems by the interpolation of cubic Hermite curves and time-parameterization along the projected paths [20]. In [8], expansion is done in a sewing-like operation where a small step is taken toward a random configuration followed by projection.

D. Visibility

We now define the notion of visibility. Let the function $\texttt{valid\_edge}(\phi_1, \phi_2)$ return *true* if the projection of a straight line edge connecting ϕ_1 to ϕ_2 using, for example, the RBS technique, is valid. The notion of visibility is defined as follows.

Definition 1. *[18] The visibility set of configuration $\phi \in \mathcal{C}_o$ is the set*

$$\mathcal{V}(\phi) = \{\phi' \in \mathcal{C}_o : \texttt{valid\_edge}(\phi, \phi') = true\}. \quad (3)$$

The visibility of a configuration is partially defined by the planning strategy and common ones are described next.

III. METHODS

In this section, we present three strategies that can be used in standard sampling-based planners. One of the methods is well known in the literature and will therefore be presented here in brief. However, the first two methods have been known in the professional community to some extent but have never been presented and analyzed properly in literature. Therefore, we will provide a broader discussion on these methods and present some novel insights.

A. Random Singularity Sampling (RSS)

Using the APC method, we can analytically generate a valid configuration with a relatively low computational cost. However, this method prevents motion between subsets of the constraint surface defined by different IK solutions. In other words, the passive chain is bounded to remain within the same IK solution and cannot pass through singular subsets separating different IK solutions. In some sense, the inability to cross singularities may be seen as an advantage when considering the problems they may cause. However, the effective workspace of the CKC is dramatically reduced. One approach to switch between different IK solutions in dual-arm manipulation is regrasping [21]. This of course requires breaking contact with one arm. In this section and the following one, we discuss two common approaches to enable a CKC to continuously pass between IK solutions while using APC.

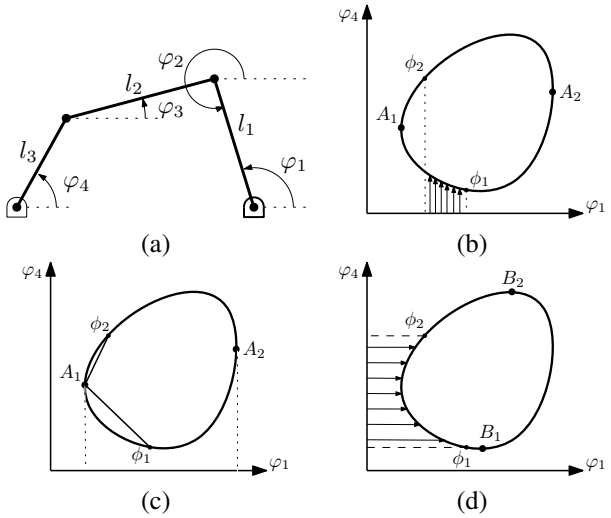

Fig. 1. (a) Four bar linkage (with four actuators) and a local connection attempt from ϕ_1 to ϕ_2 where (b) φ_1 is the active chain, (c) a singular configuration is used and, (d) φ_4 is the active chains. A_i and B_i $(i = 1, 2)$ are singular configurations when φ_1 and φ_4 are the active chains, respectively.

For a better understanding of the singularity problem, let us consider a lower dimensional example. Consider the four bar linkage seen in Figure 1a with four actuators at joints $(\varphi_1, ..., \varphi_4)$. Figure 1b illustrates a projection of the configuration space on the $\varphi_1\varphi_4$ plane. Points A_1 and A_2 are the singular points when φ_1 is selected as the active chain and joints $(\varphi_2, \varphi_3, \varphi_4)$ are the passive chain. That is, when φ_1 is set, the passive chain is imposed and defined to satisfy the closed kinematic chain constraint. The upper and lower curves connecting A_1 to A_2 correspond to the two possible IK solutions for each choice of φ_1, i.e., elbow up or elbow down of joint φ_3. In order to be able to move, all actuators need to move in a coordinated manner while satisfying the closure constraint. Now, assume we attempt to connect the configurations ϕ_1 and ϕ_2. A local connection cannot be valid while φ_1 is the active chain due to the singularity in between (A_1 or A_2). The projection of points interpolated along the φ_1-axis using IK will not connect the two configurations as seen in Figure 1b and the connection is thus not feasible.

Denote ψ_p as a subvector of $\phi \in \mathcal{C}$ corresponding to joint angles of $\mathcal{R}_p$. When $\nabla_{\psi_p} C$ is not full rank, i.e. $det(\nabla_{\psi_p} C) = 0$, the configuration is considered singular resulting in either infinite or no solutions. This type of singularity is termed *actuator singularity* as defined in [22]. These singularities are fictitious since $\mathcal{R}_p$ is not physically passive as mentioned in Section II-A. However, they impose a planning problem as described and demonstrated above. Note that $\nabla_{\psi_p} C$ is always square since the dimension of C is 3 or 6, and the dimension of ψ_p is 3 or 6 for a planar or spatial CKC, respectively.

Denote $\mathcal{D} \subset \mathcal{C}_{cl}$ as the subset corresponding to singular configurations of $\mathcal{R}_p$. The set $\mathcal{C}_a = \mathcal{C}_{cl} \backslash \mathcal{D}$ is the set of closure configurations where $\nabla_{\psi_p} C$ is full rank and is a smooth

manifold of dimension $n - n_c$ [23]. A fully actuated robotic manipulator has ξ IK solutions for a given end-effector pose. For example, a 6R spatial manipulator may have up to 16 IK solutions [24]. If the passive chain $\mathcal{R}_p$ has ξ possible IK solutions, then $\mathcal{C}_a$ is comprised of ξ *connected components*, denoted by $\mathcal{M}_k \subset \mathcal{C}_a$ $(k = 1, ..., \xi)$, which are separated by singular configurations. The notion of a connected component is somewhat similar to the self-motion manifold defined and thoroughly analyzed in [25].

A common approach to overcome this singularity problem and cross between different connected components is the explicit treatment of singular configurations. That is, singular configurations are sampled and used as bridges between connected components (Figure 1c). The singularity problem and this approach were first addressed in [15] where components in a probabilistic roadmap are connected through singular configurations. We extend this notion to single-query planners by maintaining some bias toward singular subsets in the configuration space. In the *Random Singularity Sampling* (RSS), we sample singular configurations with probability γ as target nodes in the tree's growth and enable expansion between connected components. Since these singularities are artificial and the robot is fully-actuated, the robot can later cross them.

When analyzing the RSS in terms of visibility, we observe one passive chain with ξ possible IK solutions. Given a configuration $\phi_1 \in \mathcal{M}_k$, the probability of $\phi_2 \in \mathcal{C}_{cl}$ to also be in $\mathcal{M}_k$ is $p = \mu(\mathcal{M}_k)/\mu(\mathcal{C}_{cl})$ where $\mu(\mathcal{Q})$ is the Hausdorff measure of a lower-dimensional subset $\mathcal{Q} \subset \mathcal{C}$. If we assume that $\mu(\mathcal{M}_k) = \frac{1}{\xi}\mu(\mathcal{C}_{cl})$ for all $k = 1, ..., \xi$, then we can say that $p = \xi^{-1}$. Therefore, we can set an upper bound for the measure of the visibility set by

$$\mu(\mathcal{V}(\phi)) \leq \mu(\mathcal{M}_k) = \mu(\mathcal{C}_{cl})p. \tag{4}$$

The core property of RSS is in the extended visibility of the singular configurations, where all adjacent connected components are visible. We note that this bound for the visibility is very loose and will be much lower in practical systems. Joint limits, self collisions and obstacles could dramatically obstruct visibility. Nevertheless, this bound is used to motivate the increase of visibility in the following approach.

B. Passive Chains Swap (PCS)

A different approach to address the singularity problem described in Section III-A is to swap between different passive chains available in the CKC. Referring again to the example of Figure 1, points A_1 and A_2 are the singularities when φ_1 is the active chain (Figure 1b), and points B_1 and B_2 are the singular configurations when φ_4 is the active chain (Figure 1d). A possible way to connect ϕ_1 and ϕ_2 would be to switch the role of the active chain and perform the local connection while φ_4 is the active chain. In that case, there is no passing through a singularity point (Figure 1d). The approach for connecting two points ϕ_1 and ϕ_2 would therefore be to identify the active chain producing a motion free of singularities, if available. Then, interpolate points along the straight line connecting ϕ_1 and ϕ_2, and compute for each the correct IK solution corresponding to the current active chain and common to both. This approach, termed the *Passive Chains Swap* (PCS), is known to be used by the professional community but, to the best of our knowledge, has never been addressed in literature.

From here on, let the superscript with index in parentheses $(\cdot)^{(\nu)}$ notate the affiliation to passive chain number $\nu = 1, ..., m$. Since $\mathcal{R}_p^{(i)}$ and $\mathcal{R}_p^{(j)}$ are in different locations along the CKC, the singularities of $\mathcal{R}$ with $\mathcal{R}_p^{(i)}$ as the passive chain may be different than when $\mathcal{R}_p^{(j)}$ act as the passive chain, or mathematically, $\mathcal{D}^{(i)} \neq \mathcal{D}^{(j)}$. This was demonstrated in the example in Figure 1. When $\mathcal{R}_p^{(i)}$ is the passive chain, the union of the connected components is the configuration space $\mathcal{C}_a^{(i)}$ of the chain satisfying the closure constraints and $\mathcal{R}_p^{(i)}$ is not in singularity. Now, connected components in $\mathcal{C}_a^{(i)}$ overlap connected components in $\mathcal{C}_a^{(j)}$ while including singular subsets in $\mathcal{D}^{(j)}$. When swapping the passive chain role, we alternate betweens motions in $\mathcal{C}_a^{(i)}$ to $\mathcal{C}_a^{(j)}$. Thus, the system is able to cross configurations that were previously singular, and local connections are more likely to be feasible between neighboring configurations. The idea is, therefore, to sample configurations in the ambient space and project them onto $\mathcal{C}_{cl}$ using different IK solutions of different passive chains. Then, local connection is acquired, if possible, between two configurations with the passive chain that position them in the same connected component.

In terms of visibility, a configuration $\phi \in \mathcal{C}_{cl}$ has, at most, visibility to all connected components in which it lies. By that, the set $\mathcal{V}_m(\phi)$ is the visibility set of ϕ when m passive chains are observed and is given by

$$\mathcal{V}_m(\phi) \subseteq \bigcup_{i=1}^{m} \mathcal{M}_{k_i}^{(i)} \tag{5}$$

where k_i is the corresponding IK solution index of passive chain $\mathcal{R}_p^{(i)}$. When observing multiple passive chains, we must make a distinction between dependent and independent passive chains. Two passive chains are said to be dependent if they partially overlap and their common chain has more than one IK solution. For example, consider a chain formed by a sequence of *elbow-wrist-elbow* formation [19]. In this case, one passive chain can be the *elbow-wrist* chain and the other would be the *wrist-elbow*. Each have eight IK solutions. Both share the wrist chain which is known to have more than one IK solution. Thus, they are dependent. This dependency is reflected when two configurations do not share the same IK solution for one passive chain. Consequently, this will reduce the probability for being in the same connected component for the second passive chain. In this example, setting the wrist for one passive chain determines wrist up or down resulting in the other passive chain having only four possible IK solutions. Nevertheless, if two passive chains share two joints or less (or do not share any joint), the common chain cannot have more than one solution and they would be independent. Therefore, a planar chain will never have dependent passive chains.

When considering m independent passive chains each having ξ_k $(k = 1, ..., m)$ possible IK solutions, the probability for ϕ_2 not to be in a common connected component with ϕ_1 is

$$P_m = \prod_{k=1}^{m} (1 - p_k), \tag{6}$$

where $p_k = \xi_k^{-1}$. The expression for P_m holds for any CKC with a set of m independent passive chains but does not include dependent passive chains. In order to find a better value for P_m with dependent passive chains, any given CKC must be analysed individually. The general approach would be as follows. Let $\mathcal{R}_p^{(i)}$ and $\mathcal{R}_p^{(j)}$ be two dependent passive chains of $\mathcal{R}$ with ξ_i and ξ_j IK solutions, respectively. As mentioned, the probability of two configurations not to be in the connected component corresponding to $\mathcal{R}_p^{(i)}$ is $1 - p_i$. If two configurations are not in the same connected component corresponding to $\mathcal{R}_p^{(i)}$, the probability for them to be visible through $\mathcal{R}_p^{(j)}$ decreases and is given by conditional probability to be

$$\tilde{p} = (1 - \xi_i^{-1}) \frac{1}{(\xi_j - \xi_{ij})}, \tag{7}$$

where ξ_{ij} is the number of IK solutions canceled by the common (overlapping) chain. This is because, when setting a configuration for $\mathcal{R}_p^{(i)}$, some IK solutions for $\mathcal{R}_p^{(j)}$ become impossible. Consequently, (6) is now extended to consider both dependent and independent passive chains. The probability for two configurations not to be in common connected components of m passive chains is

$$P_m = \prod_{k=1}^{m_1} (1 - p_k) \prod_{k=1}^{m_2/2} (1 - \tilde{p}_k), \tag{8}$$

where m_1 and m_2 are the number of independent and dependent passive chains, respectively, such that $m = m_1 + m_2$. Therefore, we can finally state that the visibility set of a configuration $\phi \in \mathcal{C}_{cl}$ covers up to a fraction $P_v = 1 - P_m$ of $\mathcal{C}_{cl}$, i.e.,

$$\mu(\mathcal{V}_m(\phi)) \leq P_v \mu(\mathcal{C}_{cl}). \tag{9}$$

Expressions (8)-(9) enable us to analytically find an upper bound for the measure of the visibility set with regards to the number of observed passive chains. This bound is also very loose and may be significantly reduced in the presence of joint limits and obstacles. Nevertheless, expressions (8)-(9) provide a firm motivation for increasing the number of passive chains used, especially when joint limits and collision constraints are imposed. Increasing the number of passive chains observed directly increases the visibility, i.e., increases the probability of two configurations to be connected with a single local-connection.

From the planar example to be presented in the experimental section, it is clear that the visibility increases and the runtime decreases with the addition of more passive chains. Adding more passive chains in 2D systems is straightforward. However, for a practical 3D case of dual-arm manipulation, including more passive chains in addition to the immediate ones (the arms) is considered a hard problem. Closed form IK solutions are easy to derive in special cases, such as when three consecutive axes intersect. For instance, off-the-shelf robots of six revolute joints are built such that closed form IK are easily computed. In contrast, IK solutions are hard to obtain or do not exist for arbitrary kinematic chains [26]. Analysis of the spatial case along with extended results will be presented in the experimental section.

C. Newton-Raphson (NR) projection

The use of NR projection in standard sampling-based planners has been widely used [7], [8]. Samples and interpolated points on local-connections are projected using NR and checked to satisfy all constraints. This numerical projection has been shown to be relatively expensive. Nonetheless, although analytic characterizations of visibility in the context of NR are currently unavailable, empirical results to be presented in the experimental section show high probability of two configurations to be connected.

IV. Analysis and Experimental results

This section presents an empirical performance analysis of the discussed methods for an actual robotic system. The experiments were implemented in C++ with the Open Motion Planning Library (OMPL) [27] on an Intel-Core i7-6700HQ Ubuntu machine with 8GB of RAM. Collision checking was implemented using the Proximity Query Package (PQP) [28]. The open-source code of the various experiments is available at `https://github.com/avishais/CKCplanning`.

We tested each method in six different environments. Environment *I* shown in Figure 2a consists of a 20-dimensional planner CKC with obstacles and joint limits ($[-180^o, 180^o]$). In the path planning problem of Environment *II*, shown in Figure 2b, two 6-DOF ABB IRB-120 industrial robotic arms must manipulate a rod in a collision-free path between start to the goal configurations. Environment *III*, shown in Figure 2c, requires the same robots to pass a rod through a narrow passage. Environments *IV* and *V* use two 6-DOF Comau nj-16 arms. In environment *IV* seen in Figure 2d, the robots manipulte a rod through several obstacles. Environment *V* is an industrial scene where the robots manipulate a box using suction cups from a conveyor to the mounting position. Finally, environment *VI* presents a multi-loop scenario where three Comau arms manipulate a ring between two poles. The grasps of the objects are considered rigid, and thus, the grasped object is considered part of a link in the chain. Joint limits were enforced to all industrial arms based on manufacturer data. In all environments, the defined start and goal configurations require passing through singular configurations. For each environment, we tested several sampling-based planners: the Rapidly-exploring Random Trees (RRT) [29], Bi-Directional RRT (Bi-RRT) and the Single-query Bi-directional probabilistic roadmap planner with Lazy collision checking (SBL) [30]. The Bi-RRT with projections is essentially an implementation of the Constrained Bi-RRT (CBi-RRT) in [8]. All planners are standard implementations in OMPL. In addition, the RBS technique was used to efficiently find the geodesic local connection between two configurations.

A. Experimental results

In this section we present comparative results for planning with the three discussed methods: RSS, PCS and NR. In the implementation of RSS, the planning was performed with only one passive chain. Probability γ was profiled and chosen as 0.2 to provide best performance. In all enviroments excluding *I*, PCS was implemented with the immediate passive chains

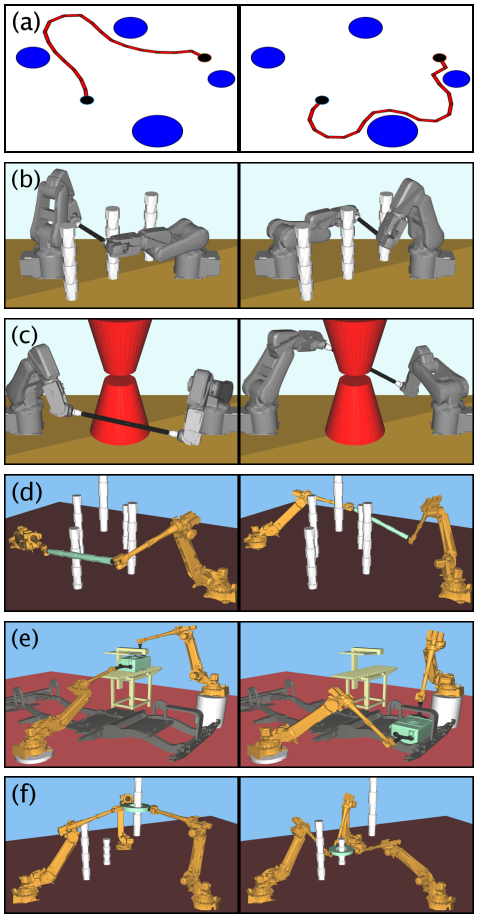

Fig. 2. The six tested environments: (a) a 20-dimensional planar CKC, two ABB robots manipulating a rod (b) between three poles and (c) through a narrow passage, two Comau arms manipulating (d) a rod and (e) a box through obstacles, and (f) three Comau arms manipulating a ring between poles.

- the arms themselves. Each arm is built in the elbow-wrist formation in which a closed-form IK solution is commonly known.

We used the Kinematics and Dynamics Library (KDL) [31] of the Open Robot Control Software (OROCOS) for the implementation of NR projections. It solves for the joint angles using Newton-Raphson for gradient descent minimization while the pseudo-inverse of the Jacobian is determined using Singular Value Decomposition (we note however that QR decomposition can generally be more efficient). Given an initial configuration in the ambient space, KDL solves the IK problem for the entire chain while enforcing the closure constraint.

In all planners, the maximum distance d from a sampled configuration in the ambient space to its nearest neighbor [6] was profiled and chosen to minimize runtime. The optimal distance $d = d_o$ is determined by the visibility, projection method and cost of local-connection derived from the method used.

It might be possible that the implementations of these strategies can be improved with additional individual or common methods such as sample-biasing and various heuristics. Nonetheless, we present them as generic as possible such that the following results provide a fundamental characterization

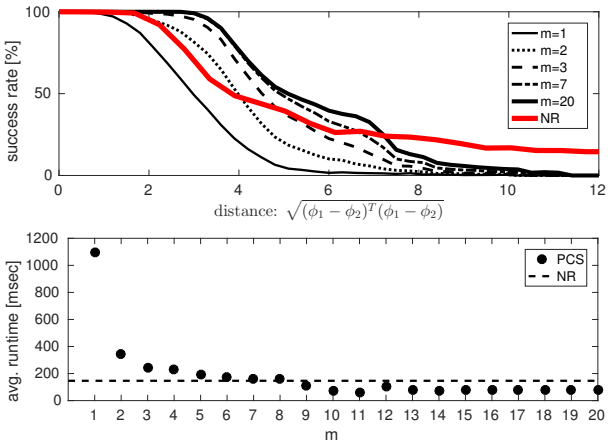

Fig. 3. Results for environment *I*. (Top) The success rate of a local-connection check with regards to the distance (bins width - 0.3) and, (bottom) runtime with regards to the number of observed passive chains m when planning with Bi-RRT.

of the methods. Figure 3 shows local-connection success rates and planning results for environment *I* with Bi-RRT, and with regards to the number of passive chains used. Table I presents the runtime performance of planning in environments *II*-*VI*. The results show an average planning time for 500 trials using each of the methods and planners. A dash mark indicates that a solution could not be found in under 1,000 seconds.

TABLE I
AVERAGE PLANNING TIME (SEC)

		RSS	PCS	NR
env. *II*	RRT	90.86	0.33	0.60
	Bi-RRT	7.27	0.22	0.13
	SBL	397.29	0.60	0.16
env. *III*	RRT	75.94	2.91	1.53
	Bi-RRT	23.10	1.06	0.92
	SBL	648.9	5.48	7.56
env. *IV*	RRT	–	99.24	75.88
	Bi-RRT	175.5	27.18	38.84
	SBL	–	147.95	234.82
env. *V*	RRT	–	–	–
	Bi-RRT	330.6	3.81	11.76
	SBL	587.29	2.61	3.55
env. *VI*	RRT	–	–	–
	Bi-RRT	537.2	3.7	36.63
	SBL	–	7.16	82.24

B. Analysis and Discussion

The planar results in Figure 3 demonstrate the benefits of visibility and projection time. As seen, the increase of passive chains for the PCS increases visibility enough above the NR's. In addition, tests show that projection time for the PCS in the planar case is about 40 times faster than NR projection. Thus, the increase of visibility combined with faster projection and local connection make the use of PCS in the planar case more beneficial.

Referring to the spatial environments, the first row in Table II shows experimental results for the visible portion P_v of $\mathcal{C}_o$ in environment *II*. These are the results of sampling 50,000 start and goal configurations in $\mathcal{C}_o$ and checking whether a local-connection is valid. However, a clearer way to understand the

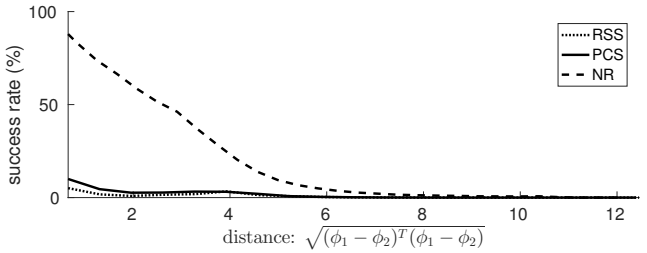

Fig. 4. The success rate of a local-connection check in environment *I* with regards to the distance between the two configurations. This corresponds to the visibility in the configuration space (bins width - 0.3).

visibility is in Figure 4 presenting the same results for environment *II* as a function of the distance between the samples. Thus, it shows the probability of a valid local connection given two configurations within some distance. PCS and RSS have a very low visibility primarily because of the low projection success rate of APC as discussed in Section II-B. On the other hand, NR has a remarkable visibility in the shorter distances. Table II also presents additional performance measures for planning with the Bi-RRT in environment *II*. Measures for the other planners and environments are relatively similar.

TABLE II
PERFORMANCE MEASURES FOR PLANNING WITH BI-RRT IN ENVIRONMENT *II*

	RSS	PCS	NR
$P_v \cdot 100\%$	0.85	1.31	23.74
max. distance d_o	0.6	1	2.6
avg. number of samples	5,544	532	151
% of failed samples	83.64	20.48	16.17
sampling % of runtime	3.03	19.05	27.80
avg. loc.-con. time (msec)	4.97	0.32	1.40
loc.-con. checks per sec	102	1,639	508
loc.-con. % of runtime	50.73	53.82	71.58
avg. number of nodes in trees	476	408	13
avg. number of nodes in path	26	29	7

It is clear that PCS and NR outperform RSS. Thus, we first begin by analyzing the reasons for which the latter perform poorly. RSS performs poorly mainly due to low visibility and the limited ability to cross singular configurations. The upper limit of the visibility for a configuration with RSS is merely the connected component it lies in. Thus, crossing to different connected components relies on the right singular sample and the distance from its nearest-neighbor. The singularities are chosen randomly and the distance to the nearest neighbor cannot be controlled. Due to the low visibility, the trees must be sufficiently large within a connected component in order to be close enough to a singular configuration. Only then is a local connection likely to be feasible. It is important to note that as the size of the trees increase, the cost of the nearest-neighbor search increases significantly and takes a larger portion of the runtime. This has a direct effect on the performance of RSS. These reasons make the RSS a non-ideal approach. Presumably, some heuristics such as biased singularity sampling and smarter projection choices can be added to speed-up the planning, but these changes are unlikely to match the PCS and NR performance.

When comparing between the NR and PCS, we pay attention to two properties: visibility and projection cost. NR is superior in visibility as seen in Figure 4 but has a relatively high projection cost. In general, the high visibility enables fast exploration and connection to the goal. This can be seen in the results of environment *II* where the configuration space is not so cluttered. However, when the configuration space is cluttered with more obstacles as in environments *IV*-*VI*, the visibility advantage of NR diminishes. In such case, extensive exploration with smaller steps is conducted resulting in many more expensive projections. PCS on the other hand already moves in smaller steps due to the low visibility but faster. We note that NR outperforms PCS in all spatial environments excluding *VI* when the obstacles are removed. We also note that the visibility affects the quality of the path in terms of smoothness. As seen in Table II, NR has the highest visibility, can move in larger steps and thus, can produce a shorter path reflected by the number of nodes it consists.

Environment *VI* is an example of a system with more than one closed kinematic chain. We note however that the analysis given in Section III-B is not fully applicable in this case. Here, for any given active chain arm there are two passive chains. Thus, a connection between two configurations is only possible when the IK solution of each passive chain is the same in both configurations. Nevertheless, we include this experiment to provide a broader benchmark. NR performs poorly in this case due to the obstacles and due to the high dimensionality resulting in significant cost of projections. The projection cost of PCS on the other hand remains low.

One issue that should also be addressed is the uniformity of the samples on the constraint manifold. While random samples in the ambient space are taken uniformly, their projection on the implicit manifold are not guaranteed to have a uniform distribution [10]. Tests on all environments have shown almost the same distribution for both projection methods, APC and NR, on the manifold. Thus, both would cover the entire manifold with the increase of samples. We should add however that when projecting a configuration, the distance from the nearest-neighbor can increase or decrease based on the projection method. Figure 5 shows the average absolute distance change between a random configuration and its projection to a valid neighbor for both methods. NR preserves the distance better than APC and is more effective in sampling within the feasible visibility region (seen in Figure 4). This advantage is also diminished in a cluttered environment.

Adding more passive chains, as seen in the planar example of environment *I*, increases the visibility and reduces planning time. This brings up the question of whether adding more passive chains, if even possible, can significantly improve the performance of PCS for the spatial case as well. As seen in Figure 4, RSS which uses only one fully actuated passive chain, has an extremely low visibility. The addition of another fully actuated passive chain in PCS was crucial to overcome the singularity problem but only nearly doubled the visibility. Thus, more passive chains would not increase the visibility significantly. In addition and as stated in Section III, finding more passive chains with closed-form IK is considered a hard problem. For example, any passive chain in the system

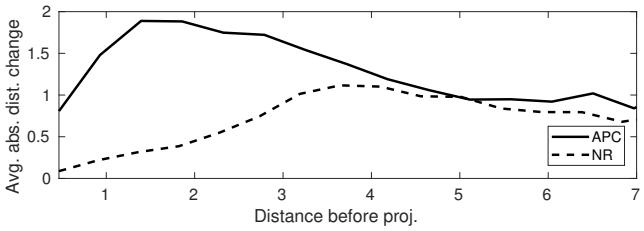

Fig. 5. Average absolute distance change between a random configuration and its projection to a valid neighbor as a function of the distance before projection, for environment *II* (bins width - 0.46).

of environments *II-IV* that includes the rod and the two adjacent joints has infinite IK solutions, and is therefore infeasible. Additional passive chains would also be dependent with limited contribution to visibility. In general, several fully actuated passive chains, which usually do not exist in actual systems, would have to be added to improve performance.

In terms of implementation, IK-based methods are hard to generalize. In both RSS and PCS, the IK of each passive chain must be explicilty and analytically defined. Implementing closed-form IK solutions for different passive chains, not to mention redundant ones, can be quite complex and in many cases impossible. In addition, singularities are generally impicitly defined and must be individually identified. This makes singularity sampling in RSS a difficult task. We also note that implementation of PCS and RSS is only possible in chains where the kinematic structure is ear-decomposable [32]. On the other hand, NR is straightforward to implement and generalize for any n-dimensional chain.

V. Conclusion

An overview and comparative analysis was introduced for common strategies of sampling-based motion planning with closed kinematic chains. We have provided an extensive review for known strategies that were not addressed previously in literature. Experimental results in several environments gave the reader a good sense of how each of the strategies perform given different planners. The above results indicate that PCS performs at least the same as NR and even better in cluttered environments. However, implementing closed-form IK solutions in PCS for different arms can be quite complex. On the other hand, NR is easier to implement and generalize for any n-dimensional chain. Future work could widen the analysis by considering other criteria such as forces within the links and joints, grasp statics, control issues and manipulability.

References

[1] C. Smith, Y. Karayiannidis, L. Nalpantidis, X. Gratal, P. Qi, D. V. Dimarogonas, and D. Kragic, "Dual arm manipulation—a survey," *Rob. and Auto. Sys.*, vol. 60, no. 10, pp. 1340 – 1353, 2012.

[2] K. Hauser, T. Bretl, J. Latombe, K. Harada, and B. Wilcox, "Motion planning for legged robots on varied terrain," *Int. Journal of Robotics Research*, vol. 27, no. 11-12, pp. 1325–1349, 11 2008.

[3] O. Khatib, K. Yokoi, K. Chang, D. Ruspini, R. Holmberg, and A. Casal, "Vehicle/arm coordination and multiple mobile manipulator decentralized cooperation," in *Proc. of the IEEE/RSJ Int. Conf. Int. Rob. and Sys.*, vol. 2, Nov 1996, pp. 546–553.

[4] J. Cortés and T. Siméon, *Sampling-Based Motion Planning under Kinematic Loop-Closure Constraints*. Berlin, Heidelberg: Springer Berlin Heidelberg, 2005, pp. 75–90.

[5] S. M. LaValle, J. H. Yakey, and L. E. Kavraki, "A probabilistic roadmap approach for systems with closed kinematic chains," in *Proc. of the IEEE Int. Conf. on Rob. and Aut.*, vol. 3, May 1999, pp. 1671–1676 vol.3.

[6] S. M. LaValle, *Planning Algorithms*. Cambridge, U.K.: Cambridge University Press, 2006, available at http://planning.cs.uiuc.edu/.

[7] M. Stilman, "Global manipulation planning in robot joint space with task constraints," *IEEE Trans. on Robotics*, vol. 26, no. 3, pp. 576–584, June 2010.

[8] D. Berenson, S. Srinivasa, D. Ferguson , and J. Kuffner, "Manipulation planning on constraint manifolds," in *Proc. of the IEEE Int. Conf. on Rob. and Aut.*, May 2009.

[9] K. Hauser, "Motion planning for legged and humanoid robots," Ph.D. dissertation, Stanford, 2008.

[10] Z. Kingston, M. Moll, , and L. E. Kavraki, "Decoupling constraints from sampling-based planners," in *Int. Sym. on Rob. Res.*, 2017.

[11] B. Kim, T. T. Um, C. Suh, and F. C. Park, "Tangent bundle RRT: A randomized algorithm for constrained motion planning," *Robotica*, vol. 34, pp. 202–225, 2016.

[12] L. Jaillet and J. M. Porta, "Path planning under kinematic constraints by rapidly exploring manifolds," *IEEE Trans. on Robotics*, vol. 29, no. 1, pp. 105–117, Feb 2013.

[13] J. H. Yakey, S. M. LaValle, and L. E. Kavraki, "Randomized path planning for linkages with closed kinematic chains," *IEEE Trans. on Rob. and Aut.*, vol. 17, no. 6, pp. 951–958, Dec 2001.

[14] L. Han and N. M. Amato, "A kinematics-based probabilistic roadmap method for closed chain systems," in *Algorithmic and Computational Robotics: New Directions (WAFR)*, D. Rus, Ed. A.K. Peters, 2000, pp. 233–245.

[15] M. Gharbi, J. Cortes, and T. Simeon, "A sampling-based path planner for dual-arm manipulation," in *Proc. of the IEEE/ASME Int. Conf. on Advanced Intelligent Mechatronics*, July 2008, pp. 383–388.

[16] A. Yershova and S. M. LaValle, *Motion Planning for Highly Constrained Spaces*. London: Springer London, 2009, pp. 297–306.

[17] M. Bonilla, E. Farnioli, L. Pallottino, and A. Bicchi, "Sample-based motion planning for robot manipulators with closed kinematic chains," in *Proc. of the IEEE Int. Conf. on Rob. and Aut.*, IEEE. Seattle, USA, 25 - 30 May: IEEE, 2015, pp. 2522 – 2527.

[18] D. Hsu, J.-C. Latombe, and H. Kurniawati, "On the probabilistic foundations of probabilistic roadmap planning," *Int. J. Rob. Res.*, vol. 25, no. 7, pp. 627–643, 2006.

[19] M. W. Spong, *Robot Dynamics and Control*, 1st ed. New York, NY, USA: John Wiley & Sons, Inc., 1989.

[20] K. Hauser, "Fast interpolation and time-optimization with contact," *Int. J. Rob. Res.*, vol. 33, no. 9, pp. 1231–1250, 2014.

[21] Z. Xian, P. Lertkultanon, and Q. C. Pham, "Closed-chain manipulation of large objects by multi-arm robotic systems," *IEEE Robotics and Automation Letters*, vol. 2, no. 4, pp. 1832–1839, Oct 2017.

[22] F. C. Park and J. W. Kim, "Singularity analysis of closed kinematic chains," *J. of Mech. Design*, vol. 121, no. 1, pp. 32 – 38, 1999.

[23] O. Bohigas, M. E. Henderson, L. Ros, M. Manubens, and J. M. Porta, "Planning singularity-free paths on closed-chain manipulators," *IEEE Trans. on Robotics*, vol. 29, no. 4, pp. 888–898, Aug 2013.

[24] D. Manocha and J. F. Canny, "Efficient inverse kinematics for general 6r manipulators," *IEEE Trans. on Rob. and Aut.*, vol. 10, no. 5, pp. 648–657, Oct 1994.

[25] J. W. Burdick, "On the inverse kinematics of redundant manipulators: characterization of the self-motion manifolds," in *Proc. Int. Conf. on Rob. and Aut.*, May 1989, pp. 264–270 vol.1.

[26] D. Manocha and J. F. Canny, "Real time inverse kinematics for general 6r manipulators," in *Proc. of the IEEE Int. Conf. on Rob. and Aut.*, May 1992, pp. 383–389 vol.1.

[27] I. A. Sucan, M. Moll, and L. E. Kavraki, "The open motion planning library," *IEEE Robotics & Automation Magazine*, vol. 19, no. 4, pp. 72–82, Dec 2012.

[28] E. Larsen, S. Gottschalk, M. C. Lin, and D. Manocha, "Fast distance queries with rectangular swept sphere volumes," in *Proc. of the IEEE Int. Conf. on Rob. and Aut.*, vol. 4, 2000, pp. 3719–3726.

[29] S. M. Lavalle, "Rapidly-exploring random trees: A new tool for path planning," Tech. Rep., 1998.

[30] G. Sánchez and J.-C. Latombe, *A Single-Query Bi-Directional Probabilistic Roadmap Planner with Lazy Collision Checking*. Berlin, Heidelberg: Springer Berlin Heidelberg, 2003, pp. 403–417.

[31] R. Smits, "KDL: Kinematics and Dynamics Library," http://www.orocos.org/kdl.

[32] D. Xie and N. M. Amato, "A kinematics-based probabilistic roadmap method for high dof closed chain systems," in *Proc. of the IEEE Int. Conf. on Rob. and Aut.*, vol. 1, 2004, pp. 473–478.